Control of Offshore MMC during Asymmetric Offshore AC Faults for Wind Power Transmission

Lei Shi, Grain Philip Adam, *IEEE Member*, Rui Li and Lie Xu, *IEEE Senior Member*

***Abstract*— The adoptions of medium-voltage in AC collection networks of large DC connected wind farms significantly increase the AC current magnitudes during normal and fault conditions. Controlling fault currents at zero during asymmetric AC faults is possible, but it has several drawbacks such as increased risk of protection mal-operation due to absence of fault currents, which also tends to prevent the recovery of AC voltage in post-fault. Therefore, this paper presents an enhanced control strategy that exploits the induced negative sequence voltages to facilitate controlled injection of negative sequence currents during asymmetric AC faults. The proposed control not only defines a safe level of fault current in the offshore AC network but also instigates immediate recovery of the AC voltage following clearance of AC faults, which avoid protection mal-operation. In addition, the positive sequence voltage set-point of the offshore modular multilevel converter (MMC) is actively controlled by considering the negative and zero sequence voltages, which effectively avoids the excessive overvoltage in the healthy phases during asymmetrical AC faults. The theoretical basis of the proposed control scheme is described, and its technical viability is assessed using simulations.**

I. Introduction

To date, there are large amount of offshore wind powers already installed in Europe and many new plants are under construction or at planning stage [1]. Among several transmission system technologies, voltage source converter (VSC) based high voltage DC (HVDC) transmission technology offers a cost-effective solution for connecting remote offshore wind farms (OWFs) and a number of such schemes are already in operation [2, 3].

The use of double-synchronous reference frame for control of conventional VSCs, where the AC voltages and currents are decomposed into positive and negative sequence components, improves the VSC behaviors during asymmetrical faults and is well documented in [4-7]. These works have investigated a number of achievable operational objectives during unbalanced AC voltages and asymmetric AC faults when negative sequence components are regulated, e.g. suppression of negative sequence currents (for maintaining balanced AC currents), nullification of oscillating active power (for prevention of injection of double frequency oscillating power into DC side), and maximization of active power transfer. An enhanced dynamic voltage control for type 4 wind turbines (WTs) is presented in [8], which employs both positive and negative sequence voltages to prevent excessive rise of the AC voltage in the healthy phases during distant asymmetric AC faults. The effectiveness of the presented voltage control is demonstrated when the WTs operate as part of a synchronous AC grid. Particularly, it can maintain the voltage magnitudes of the healthy phases nearby the WTs around 1.0 pu, while minimize the voltage depression in the faulty phases. In [9, 10], the potential impact of the control methods that exploit negative sequence components on onshore AC grid codes are further reviewed. However, the impact on power electronics dominated power systems such as AC network of HVDC connected OWFs need to be further investigated.

Reference [11] proposed a control strategy for riding through less severe asymmetric AC faults in the offshore network of HVDC connected wind farm, where both WTs and offshore two-level HVDC converter control their negative sequence current injected into offshore AC network in order to eliminate the oscillating AC power at their respective filter buses. This approach aims to minimize the DC side voltage and current ripples. During severe asymmetric AC faults or when the ratio between the negative sequence voltage and the positive sequence voltage exceeds 70%, the negative sequence current controllers of the WTs and offshore HVDC converter are disabled [10]. Nonetheless, disabling of the negative sequence current controllers may expose semiconductor switches of the converters to excessive current stresses due to unrestrained negative sequence currents. Further investigation conducted in [12] reveals that the reactive current injection during faults curtails the delivered active power and the ability to mitigate the oscillating term from DC side, while only has limited impact on the offshore grid voltage during faults. Due to serval constraints posed by the converters, the characterization of negative sequence current for offshore AC grid fault behaviors becomes increasingly important, particularly from the

This project has received funding from the European Union's Horizon 2020 research and innovation programme under grant agreement No 691714.

The authors are with the Department of Electronic and Electrical Engineering, University of Strathclyde, Glasgow, G1 1XW UK (e-mail: lei.shi@strath.ac.uk, grain.adam@strath.ac.uk, rui.li@strath.ac.uk, lie.xu@strath.ac.uk).

protection point of view [1, 13, 14].

Unlike two-level VSCs, several studies on the behavior of modular multilevel converters (MMCs) under asymmetric AC faults reveal that a well-controlled MMC does not inject even harmonic currents into DC side thus exhibits no even harmonic voltage ripples in the DC link voltage when it operates with balanced or unbalanced AC currents and voltages [15-17]. Therefore, the previous objective of eliminating the oscillating components of the active power during asymmetric faults becomes redundant. The negative sequence currents represent an additional degree of freedom that could be exploited to optimize overall system transient behavior in conjunction with other protection considerations.

To facilitate the analysis of asymmetrical faults, power circuits are generally decomposed into equivalent positive, negative and zero sequence circuits [18]. Reference [19] adopts controlled current sources to represent VSCs in sequence network when analyzing asymmetrical AC faults. However, a fundamental problem of the representation in [19] is the absence of shunt impedances across the current sources of the sequence networks, which are necessary for decoupling of the current sources from the leakage inductances of the converter transformer and phase interfacing inductors. This has led to circuit anomaly and resulted in extremely high voltages when negative sequence currents are suppressed as in [18]. It is well understood that injecting appropriate negative sequence voltage regulates negative sequence current during asymmetrical AC faults. Therefore, the current source representation is abandoned in this paper and controlled voltage source equivalent is adopted as in [20]. Such an approach is preferred because it does not require any factitious impedance as pointed out earlier in the current source representation.

Based on the findings of the sequence networks, the complete suppression of negative sequence currents by the offshore MMC and WT converters leads to problematic behaviour. Thus, an enhanced AC fault ride-through scheme that employs negative sequence voltage and current control is proposed to achieve defined safe fault current level and enable fast post-fault AC voltage recovery for effective and speedy fault detection and discrimination. The positive sequence voltage set-point of the offshore MMC is actively controlled by considering the negative and zero sequence voltages, which effectively avoids overvoltage of the offshore network and over-modulations of offshore MMCs during asymmetrical faults.

The rest of the paper is organized as follows: Section II develops sequence networks in phasor domain to analyze and highlight the potential issues that may arise during asymmetric AC faults in HVDC connected OWF AC network. Section III proposes an enhanced control strategy that exploits negative sequence current and voltage to explicitly control the fault current level and prevent healthy phases' overvoltage during asymmetric AC faults. Validity of the proposed solution is confirmed by numerical simulations in section IV. Section V explores potential applications of the proposed scheme in protection and fault current handling and distributions at WT cluster level. Finally, conclusions are drawn in section VI.

II. Sequence Network Analysis of HVDC Connected Offshore Wind Farm AC Grid

To simplify the analysis and for the purpose of illustration, the offshore AC collection grid with an AC fault applied at the 66 kV offshore cable shown in Fig. 1 is reduced to Fig. 2, where the offshore MMC and WT converters in Fig. 1 are replaced by two controllable three-phase voltage sources. E_{MMC}^{k} and I_{MMC}^{k} (k=a, b, and c) are the phase voltage and current of the offshore MMC station, respectively; E_{WT}^{k} and I_{WT}^{k} are the respective phase voltage and current of the WT; V_F^k and I_F^k are the voltage and current at the fault point, respectively; Z_{MMC} and Z_{WT} are the equivalent impedances on the offshore MMC and WT sides, respectively; and the fault impedance is Z_F. The switches shown in Fig. 2 are manipulated to represent different fault scenarios to be considered. For an example, a single-phase-to-ground fault can be represented by closing SW_F^a and SW_F^G.

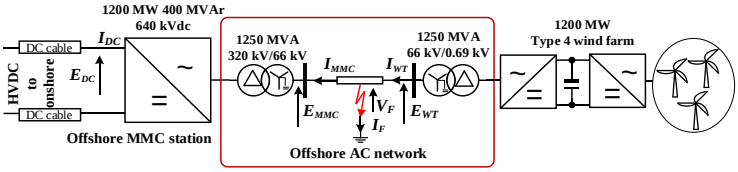

Fig. 1 Generic representation of offshore network.

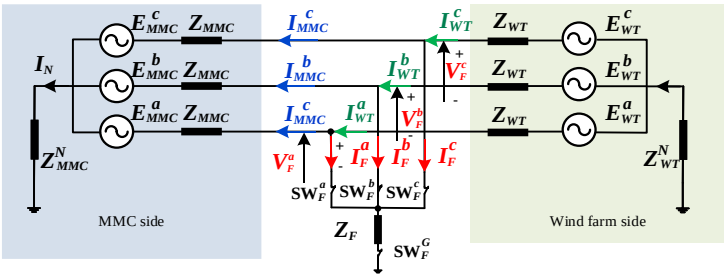

Fig. 2 Simplified offshore AC grid during faults.

The generic phasor expressions that describe the equivalent circuit of the OWF in Fig. 2 are:

$$\begin{cases} \mathbf{E}_{MMC}^{abc} + \mathbf{Z}_{MMC} \cdot \mathbf{I}_{MMC}^{abc} = \mathbf{V}_F^{abc} \\ \mathbf{E}_{WT}^{abc} - \mathbf{Z}_{WT} \cdot \mathbf{I}_{WT}^{abc} = \mathbf{V}_F^{abc} \end{cases} . \quad (1)$$

The voltage and current vectors at potential fault point 'F' are:

$$\begin{cases} \mathbf{V}_F^{abc} = \mathbf{Z}_F \cdot \mathbf{I}_F^{abc} \\ \mathbf{I}_F^{abc} = \mathbf{I}_{WT}^{abc} - \mathbf{I}_{MMC}^{abc} \end{cases} \quad (2)$$

where $\mathbf{E}_{WT}^{abc}$, $\mathbf{E}_{MMC}^{abc}$ and $\mathbf{V}_F^{abc}$ are column vectors of the aggregate wind farm converter and MMC terminal voltages and the voltage at fault point, respectively; $\mathbf{I}_{WT}^{abc}$, $\mathbf{I}_{MMC}^{abc}$ and $\mathbf{I}_F^{abc}$ are column vectors of the wind farm converter and MMC currents and the fault current, respectively; and $\mathbf{Z}_{MMC}$ and $\mathbf{Z}_{WT}$ are generically defined, with 'x' referring to 'MMC' and 'WT' as:

$$\mathbf{Z}_x = \begin{bmatrix} Z_x + Z_x^N & Z_x^N & Z_x^N \\ Z_x^N & Z_x + Z_x^N & Z_x^N \\ Z_x^n & Z_x^N & Z_x + Z_x^N \end{bmatrix} . \quad (3)$$

In (3), N denotes grounding impedance. Recall that the symmetrical component transforms three-phase a, b, c variables $\mathbf{F}^{abc}$ into equivalent variables $\mathbf{F}^{0+-}$ in sequence frame by:

$$\begin{cases}\mathbf{F}^{abc}=\mathbf{A}\mathbf{F}^{0+-}\\ \mathbf{F}^{0+-}=\mathbf{A}^{-1}\mathbf{F}^{abc}\end{cases} \tag{4}$$

where the transformation matrix $\mathbf{A}$ is:

$$\mathbf{A}=\begin{bmatrix}1&1&1\\1&\alpha^2&\alpha\\1&\alpha&\alpha^2\end{bmatrix}\quad and\quad \mathbf{A}^{-1}=\frac{1}{3}\begin{bmatrix}1&1&1\\1&\alpha&\alpha^2\\1&\alpha^2&\alpha\end{bmatrix} \tag{5}$$

where $\alpha=1\angle 120°$. After transforming (1) to sequence frame using (4) and (5), the following expressions are obtained:

$$\begin{cases}\mathbf{E}_{MMC}^{0+-}+\mathbf{Z}_{MMC}^{0+-}\cdot\mathbf{I}_{MMC}^{0+-}=\mathbf{V}_F^{0+-}\\ \mathbf{E}_{WT}^{0+-}-\mathbf{Z}_{WT}^{0+-}\cdot\mathbf{I}_{WT}^{0+-}=\mathbf{V}_F^{0+-}\end{cases} \tag{6}$$

where $\mathbf{Z}_x^{0+-}=\mathbf{A}^{-1}\mathbf{Z}_x\mathbf{A}$ is a diagonal matrix and its components are: $Z_x^{\,0}=Z_x+3Z_x^{\,n}$, and $Z_x^{\,+}=Z_x^{\,-}=Z_x+Z_x^{\,n}$. Expanding (6) leads to three pairs of decoupled equations which can be expressed graphically as three independent circuits for positive, negative and zero sequence voltages and currents. It should be noted that for converter-based networks, the negative sequence quantities can be controlled by injecting negatives sequence voltage through corresponding controllers, while, the zero sequence is blocked by the delta-start transformer connection from converter side. Thus, compared with the traditional sequence modelling [18], the negatives sequence voltages are modelled to assess the behaviours during asymmetrical AC faults.

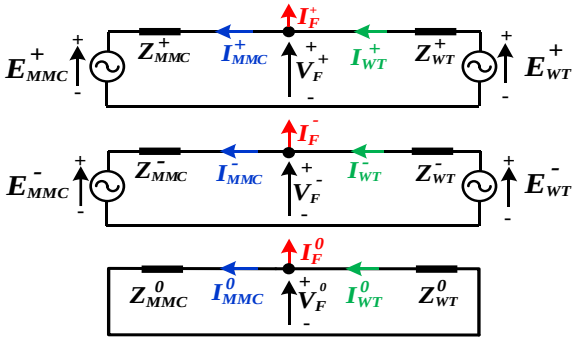

Fig. 3 Sequence network during normal operation.

Similarly, the sequence voltages at the fault point are

$$\mathbf{V}_F^{0+-}=\mathbf{Z}_F^{0+-}\cdot\mathbf{I}_F^{0+-} \tag{7}$$

where $\mathbf{Z}_F^{0+-}$ is a diagonal matrix of fault impedances. From (6) and (7), considering all the four switches in Fig. 2 are open which gives open circuit for fault path, three independent positive, negative and zero sequence networks can be obtained as shown in Fig. 3.

A. Single-phase-to-ground faults

When a single-phase-to-ground AC fault occurs in phase a as represented by closing the switches SW_F^a and SW_F^G in Fig. 2, the main constraints that define the fault behaviors are: fault currents in the healthy phases (b and c) are zero, so phase a is the contributor to the fault current and the voltage at fault point in the faulty phase a is merely determined by fault impedance Z_F. These hypotheses are expressed mathematically as:

$$V_F^{\,a}=Z_F^{\,a}I_F^{\,a}\Rightarrow V_F^{\,0}+V_F^{\,+}+V_F^{\,-}=Z_F^{\,a}(I_F^{\,0}+I_F^{\,+}+I_F^{\,-}) \tag{8}$$

$$\begin{cases}I_F=I_F^a=I_F^0+I_F^+ +I_F^-\\ I_F^b=0\Rightarrow I_F^0+\alpha^2 I_F^+ +\alpha I_F^-=0\,.\\ I_F^c=0\Rightarrow I_F^0+\alpha I_F^+ +\alpha^2 I_F^-=0\end{cases} \tag{9}$$

After algebraic manipulation of (9) and (10), it yields:

$$\begin{cases}I_F^0=I_{WT}^0-I_{MMC}^0=I_F^+=I_{WT}^+-I_{MMC}^+=I_F^-=I_{WT}^--I_{MMC}^-=\frac{1}{3}I_F^a\\ V_F^0+V_F^+ +V_F^-=I_F^aZ_F=3I_F^0Z_F=3I_F^+Z_F=3I_F^-Z_F\end{cases} \tag{10}$$

From the properties of series circuit exhibited in (10), the sequence network for a single-phase-to-ground AC fault is drawn as shown in Fig. 4. Notice that the sequence network in Fig. 4 is similar to that of the conventional synchronous AC power system, except it includes negative sequence voltage that can be injected into the offshore AC network by offshore MMC and WT converters.

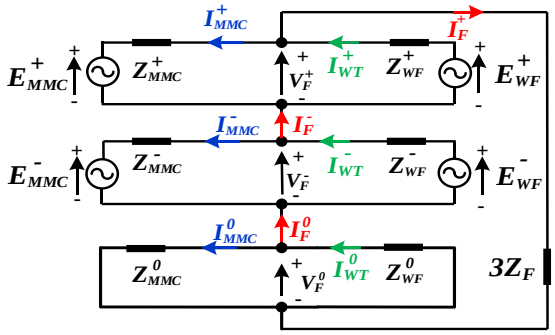

Fig. 4 Equivalent sequence circuits during single-phase-to-ground faults.

From (10), the fault current becomes:

$$I_F^{\,a}=3(I_{WT}^{\,0}-I_{MMC}^{\,0})=3(I_{WT}^{+}-I_{MMC}^{+})=3(I_{WT}^{-}-I_{MMC}^{-}). \tag{11}$$

From the above analysis of single-phase faults, the following observations are drawn:

- When the offshore MMC and WT control their output negative sequence currents at zero, i.e. $I_{WT}^{-}=I_{MMC}^{-}=0$, based on (11), fault current will become zero ($I_F^a=0$), and MMC and WT positive sequence currents must be equal ($I_{WT}^{+}=I_{MMC}^{+}$), contributing in their entireties to power transfer. Furthermore, (11) entails that the MMC and WT zero sequence currents will vanish regardless of their transformer ground arrangements, i.e. $I_{WT}^{\,0}=0$ and $I_{MMC}^{\,0}=0$.
- When the WT converter controls its negative sequence current at zero ($I_{WT}^{-}=0$), while MMC does not ($I_{MMC}^{-}\neq 0$), (11) indicates that the MMC alone defines the fault current level, i.e. $I_F^{\,a}=3I_{MMC}^{-}$. Under such an operating condition, the MMC negative sequence current defines the difference between zero and positive sequence currents of the MMC and WT, i.e. $I_{WT}^{\,0}-I_{MMC}^{\,0}=I_{WT}^{+}-I_{MMC}^{+}=-I_{MMC}^{-}$. Hence, a certain proportion of the positive sequence current will not contribute to power

transfer.

Fig. 5 shows selected results to substantiate the analysis and observations drawn above, assuming a single-phase-to-ground AC fault from 2.5 s to 2.64 s at the offshore AC cable as shown in Fig. 1. Observe that the WT and MMC currents shown in Fig. 5 (b) and (c) remain balanced during the single-phase-to-ground AC fault (after the initial transients) and consist of positive sequence components only as revealed in the above analysis. The fault current in Fig. 5 (d) decays rapidly to zero as soon as cables discharge, resulting in disappearance of zero sequence currents as established above. Notice that when the fault is cleared, the negative sequence voltages, which are injected by WT and MMC to suppress the negative sequence current and can be quantified by $E_{MMC}^{-}=E_{WT}^{-}=V_{F}^{-}$ from Fig. 4, remain. This is because after fault clearance, the boundary condition as depicted by (10) does not exist, which separates the sequence networks into the original three independent circuits as shown in Fig. 3. To keep the AC currents of the offshore MMC and WTs balanced, the residual negative sequence voltages remain equal and unchanged. This behaviour prevents AC voltage recovery after fault clearance at 2.64 s as shown in Fig. 5 (a).

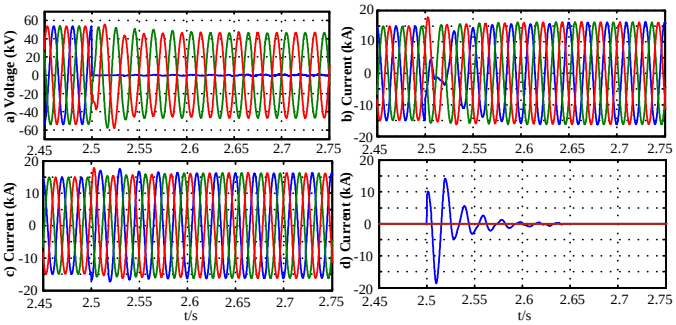

Fig. 5 Simulation waveforms during single-phase-to-ground fault from 2.5 s to 2.64 s when both MMC and WT suppress their negative sequence currents to zero: (a) grid side voltages (E_{MMC}), (b) MMC grid side three-phase currents (I_{MMC}), (c) WT three-phase currents (I_{WT}), (d) fault currents (I_F).

B. *Phase-to-phase AC faults*

When a phase-to-phase AC fault is considered between phases *b* and *c* as depicted by closing the switches SW_F^b and SW_F^c, and assuming the fault impedance of Z_F, the main constraints are:

$$V_F^c = V_F^b + Z_F I_F^b \tag{12}$$

$$I_F^a = 0, \qquad I_F^b + I_F^c = 0. \tag{13}$$

From (12) and (13), the positive and negative sequence current and voltage relationships are deduced:

$$\begin{cases} I_F^+ = -I_F^- \Rightarrow I_{WT}^+ - I_{MMC}^+ = -(I_{WT}^- - I_{MMC}^-) \\ I_F^0 = I_{WT}^0 - I_{MMC}^0 = 0 \end{cases} \tag{14}$$

$$V_F^+ = V_F^- - I_F^- Z_F. \tag{15}$$

Based on the properties exhibited by (14) and (15), the equivalent sequence network for a phase-to-phase AC fault is drawn as shown in Fig. 6. Notice that the sequence network in Fig. 6 differs from the conventional synchronous AC network due to the presence of negative sequence voltages which are injected into the offshore AC grid by the WT and MMC, and it is in line with that presented in [20]. Based on the above analysis of phase-to-phase AC fault, its behaviors are similar to the single-phase-to-ground AC fault established earlier. That is, no fault current will be observed when both offshore MMC and WT suppress their negative sequence currents, i.e. $I_F^+ = -I_F^- = 0$, $I_{WT}^- = I_{MMC}^- = 0$ and $I_{WT}^- = I_{MMC}^- = 0$. Also, operation under such condition leads to residual negative sequence voltage which prevents AC voltage recovery in post-fault. Because of similarity, no quantitative validation of the analysis of the phase-to-phase AC fault is presented.

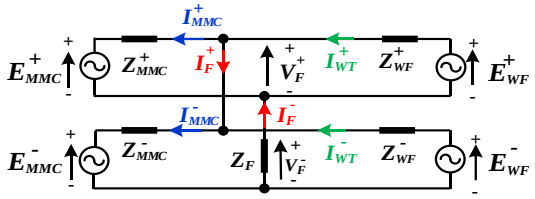

Fig. 6 Equivalent sequence circuit during phase-to-phase fault.

C. *Phase-to-phase-to-ground AC faults*

When a double phase-to-ground fault occurs in phase *b* and *c* as graphically depicted by closing the switches SW_F^b, SW_F^c and SW_F^G, the fault behavior can be described by:

$$V_F^b = V_F^c = Z_F(I_F^b + I_F^c) = 3Z_F I_F^0 \tag{16}$$

$$I_F^a = I_F^0 + I_F^+ + I_F^- = 0. \tag{17}$$

After algebraic manipulation of (19) and (20), it yields:

$$I_F^0 + I_F^+ + I_F^- = I_F^a = 0 \tag{18}$$

$$V_F^+ = V_F^- = V_F^0 - 3Z_F I_F^0 \tag{19}$$

$$I_F = I_F^b + I_F^c = 3I_F^0. \tag{20}$$

Based on circuit properties depicted by (18), (19) and (20), the sequence network for a phase-to-phase-to-ground AC fault is drawn in Fig. 7 where the positive, negative and zero sequence components co-exist as in the conventional synchronous AC power network. As in previous cases, the inclusion of negative sequence voltages of the offshore MMC and WTs has resulted in the following possibilities:

- Suppression of negative sequence currents at MMC and WT $(I_{WT}^- = I_{MMC}^- = 0)$ can only ensure zero negative sequence fault current $(I_F^- = 0)$ as shown in Fig. 7, but does not lead to zero fault current as in previous fault cases according to (19). This is because the network in Fig. 7 permits the residual positive sequence voltage at fault point to define both negative and zero sequence voltages. This means the fault current will be defined merely by residual positive sequence voltage at fault point and effective impedance in the zero sequence path, as depicted by (19). Under such condition, positive and zero sequence currents, and the fault current follow the relationship: $I_F^0 = -I_{WT}^0 + I_{MMC}^0 = I_{WT}^+ - I_{MMC}^+$, which entails the fault current and the net zero sequence current in the offshore AC network is determined by the net contribution from the positive sequence current. Therefore, it can deduce that lowering positive sequence voltage (and hence lower positive sequence current) will

lead to lower zero sequence current, hence fault current level.

- The equal imposition of positive, negative and zero sequence voltages dictated by the parallel nature of sequence networks during phase-to-phase-to-ground AC faults will result in overvoltage in the healthy phase as $V_F^a = V_F^+ + V_F^- + V_F^0$. Thus, due to the presence of negative sequence voltage, it is necessary to reduce the positive sequence voltage to prevent both excessive overcurrent and overvoltage in the offshore AC grid.

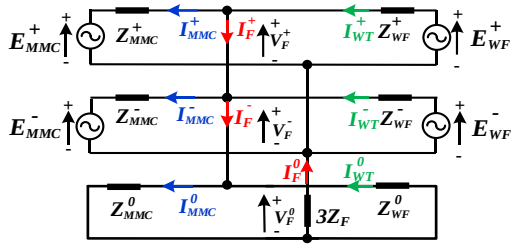

Fig. 7 Equivalent sequence circuit during double-phase-to-ground faults.

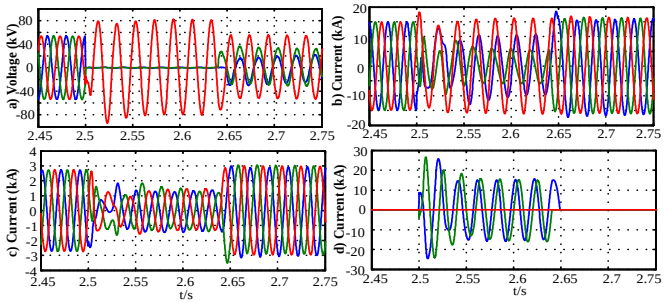

Fig. 8 Simulation waveforms for phase-to-phase-to-ground fault occurring at 2.5 s and self-cleared at 2.64 s when both MMC and WT suppress their negative sequence currents to zero: (a) grid side voltages (E_{MMC}), (b) MMC grid side currents (I_{MMC}), (c) MMC converter side currents (I_{CMMC}), (d) fault currents (I_F).

Fig. 8 shows selected simulation waveforms during the offshore phase-to-phase-to-ground fault from 2.5 s and to 2.64 s to validate the above analysis. Fig. 8 (c) shows the MMC currents measured at the converter side remain balanced with reduced magnitude and contain no zero sequence component, while that measured at grid side in Fig. 8 (b) exhibit sustained unbalance due to zero sequence component. The three-phase fault currents as shown in Fig. 8 (d) are no longer zero. Notice that the significant overvoltage in the healthy phase is observed during the fault as shown in Fig. 8 (a), which is due to the induced zero and negative sequence voltages as aforementioned. After fault clearance, the negative sequence voltage remains unchanged and the currents are balanced as shown in Fig. 8 (b) whereas the zero sequence voltage disappears. These residual negative sequence voltages prevent the recovery of the offshore network as shown in Fig. 8 (a), which is similar to the previously discussed single-phase-to-ground fault.

III. Proposed Scheme for Offshore AC Fault Management

From the anomalies revealed in the above discussions, the previous negative sequence suppression control, which regulates the negative sequence current from both the MMC and WTs to be zero, is inadequate and thus, a modified approach that exploits the inherent characteristics imposed by the sequence networks developed in section II to control fault currents in offshore AC network is proposed to achieve the following objectives:

1) Enable fault detection and discrimination by defining safe fault current level.
2) Prevent excessive overvoltage in the offshore AC network.
3) Accelerate offshore AC voltage recovery following clearance of asymmetric AC faults.

A. Proposed fault current management scheme

To address the problems highlighted above, the offshore MMC is equipped with outer negative sequence AC voltage controllers as shown in Fig. 9 which regulate both direct and quadrature components of the negative sequence voltage to zero during normal operation, and provide controlled negative sequence currents into offshore AC network during offshore asymmetrical AC faults.

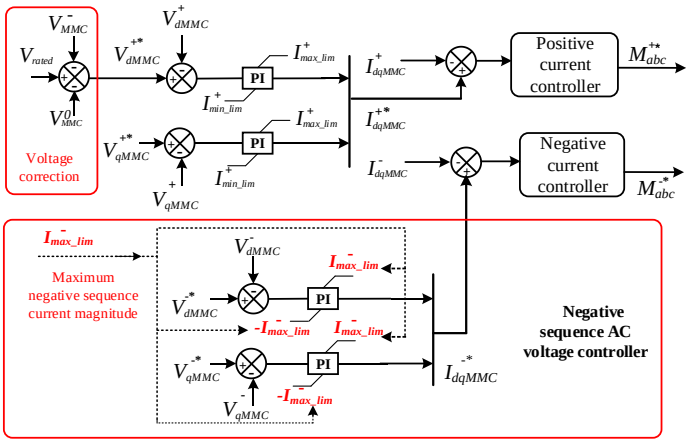

Fig. 9 Modified control strategy for offshore MMC stations.

As established in section II, the magnitude of the fault current is determined by the negative sequence current that is injected by the offshore MMC or WT during asymmetrical faults. Therefore, WTs suppress their negative sequence currents during these asymmetric AC faults and the offshore MMC exclusively defines the fault current level for protection purpose by controlling the injected negative sequence currents. According to the theoretical analysis in section II and control scenario stated above, the fault currents during single-phase-to-ground and phase-to-phase AC faults are linked to MMC negative sequence current by the following relationships: $I_F^a = 3I_{MMC}^-$ and $I_F^a = -I_F^b = j\sqrt{3}I_F^- = j\sqrt{3}I_{MMC}^-$ respectively as demonstrated quantitatively by Fig. 10 (a) and (b). Generally, during asymmetrical AC faults, the negative sequence current injected by MMCs is insufficient to correct the unbalanced grid voltage. Therefore, the outer negative sequence AC voltage controller shown in Fig. 9 should not pursue the objective of suppression of negative sequence voltage to zero. Instead, it defines a safe level of negative sequence current set by the maximum negative sequence current magnitude $I_{\max\_lim}^-$. The injected negative sequence current should also be compatible

with protection system requirements. Thus, $I^{-}_{\max\_lim}$ must account for circuit breaker settings and ratings of individual lines.

During post-fault, the offshore MMC will facilitate controlled injection of negative sequence current in an effort to nullify the residual negative sequence voltages created by the fault to accelerate AC voltage recovery, while the WT converters keep negative sequence current at zero. It must be emphasized that the magnitude and characteristics of the injected negative sequence current impact the AC voltage recovery speed. Injection of small negative sequence current leads to slow nullification of residual negative sequence voltage after fault clearance, as will be demonstrated in the simulation studies.

Based on principles articulated above, cascaded *d-q* negative sequence voltage and current loops are designed to facilitate controlled injection of negative sequence current by the offshore MMC, with *d-q* negative sequence current orders are given equal priorities as determined by $I^{-}_{\max\_lim}$ as shown in Fig. 9.

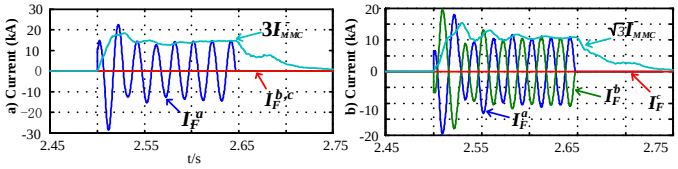

Fig. 10 Simulation waveforms for illustrating the relationship between fault current magnitude and corresponding injected negative sequence current: (a) single-phase-to-ground fault, (b) phase-to-phase fault.

B. Over-modulation and overvoltage consideration for offshore MMC stations

During phase-to-phase-to-ground AC faults, the magnitudes of zero sequence current and voltage depend on residual positive sequence voltage, and the simultaneous co-existence of positive, negative and zero sequence voltages could potentially create significant overvoltage in the healthy phase on the grid side. Also, when negative sequence currents are no longer controlled at zero during single-phase-to-ground AC faults, zero sequence voltage is induced, which will also exacerbate the overvoltage problem in the healthy phases.

In addition, the required converter output voltage is the sum of negative and positive sequence components generated by their corresponding inner current controllers. Trying to maintain the positive sequence voltage at nominal value in the presence of negative sequence voltage during asymmetrical AC faults will lead to the total required voltage over the converter voltage limitation [21] and the saturation of both positive and negative control loops. This over-modulation behaviour degrades the controllability of the system and thus should be avoided.

Therefore, to prevent overvoltage in the offshore AC network and converter over-modulation, this paper introduces an adjustment to the positive sequence voltage set-point of the offshore MMC that takes into account both induced negative and zero sequence voltages as shown in the top left of Fig. 9. Thus, a further modification that describes the positive sequence voltage set-point is:

$$V^{+*}_{dMMC} = V_{rated} - V^{-}_{MMC} - V^{0}_{MMC}\,. \tag{21}$$

By applying (21), reduction of the positive sequence voltage magnitude in the offshore AC network will be initiated by the MMC to prevent overvoltage in the AC grid during asymmetric AC faults. In the meantime, the reduction of positive sequence voltage also prevents the saturation of the voltage and current controllers and the over-modulation of the converter to ensure controllability of the system.

IV. Simulations

To validate the analysis and effectiveness of the proposed methods in section II and III, the system shown in Fig. 11 is simulated in PSCAD/EMTDC. The system consists of a 1200 MW OWF, local 66 kV offshore AC collection grid and an MMC based HVDC system rated at ±320 kV to transfer power to the onshore grid. A simple voltage source is used to represent the onshore AC grid, while offshore and onshore MMC1 and MMC2 are represented using electromagnetic Thevenin equivalent model with 350 submodules per arm available in PSCAD library [22, 23]. MMC1 controls the offshore AC voltage while MMC2 regulates the DC voltage of the HVDC link. The OWF is composed of 4 clusters and each is rated at 300 MW and is modelled as a lumped converter, as illustrated in Fig. 11. Different AC cables are used to reflect different distances of the WT converters from offshore PCC. This work models DC cables by detailed frequency dependent tool in PSCAD, in which the cable electrical parameters such as *R*, *L* and *C* are internally determined by physical dimension, insulation layers, etc [24]. Relatively, short AC cables of the offshore windfarm are modelled by simple PI sections with the following electrical parameters: *R*=10 mΩ/km, *L*=0.3 mH/km and *C*=0.4 μF/km [25]. AC circuit breakers (ACCBs) are installed at end of each cluster cable to clear the faulty cluster from the wind farm based on overcurrent, as will be discussed in section V. The leakage inductances of all the transformers used in the model are 0.18 pu. Only the WT grid side converters are modelled, which include the following controllers: active power, reactive power, and positive and negative sequence current controllers.

The test system is subjected to a temporary asymmetric AC faults F_1 at the middle of the cable C5 at *t*=2.5 s, with fault duration of 140 ms and fault resistance of 0.1 Ω. It is assumed that each WT converter is equipped with a DC chopper to dissipate excess energy during offshore AC faults.

As discussed in previous sections, during asymmetric AC faults, the WT converters control their negative sequence currents at zero whereas the maximum negative sequence current contribution from the offshore MMC is limited to 0.25 pu, considering the need for fault detection and post-fault recovery though it can be set to different values based on system control and protection requirements.

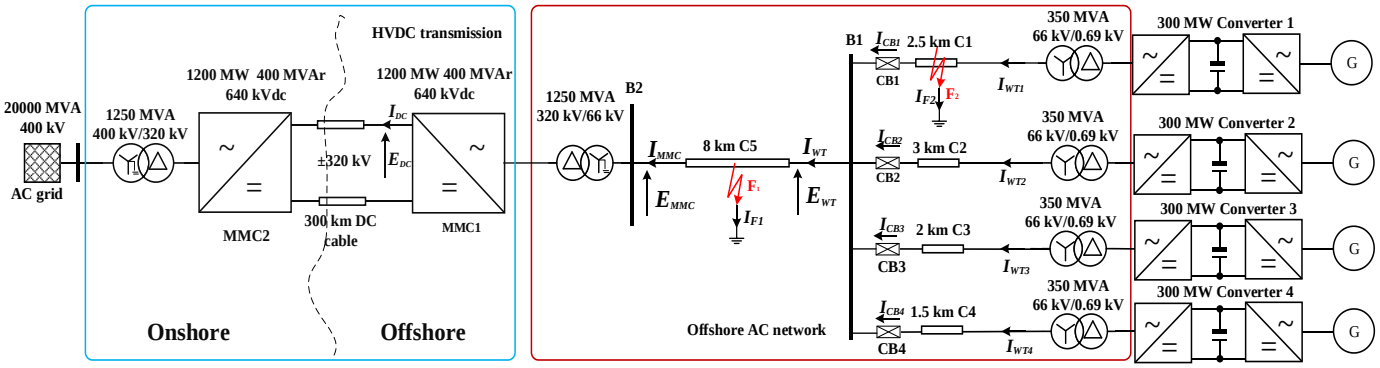

Fig. 11 The detailed representation of offshore network.

A. *Single-phase-to-ground faults*

Fig. 12 displays simulation waveforms during a single-phase-to-ground fault (F1, Fig. 11) at cable C5, whereas Table 1 lists the sequence of the events. Unlike the illustrative case presented in Fig. 5, Fig. 12 (a) shows that the AC voltage in the offshore AC network has recovered to pre-fault level 60 ms after fault clearance. During the fault period, Fig. 12 (b) shows that the currents injected to the 66 kV offshore network by the MMC contain negative sequence currents, which feed the fault currents shown in Fig. 12 (e). Due to the use of star-delta interfacing transformer, the zero sequence currents are absent on converter side and thus the converter side currents exhibit different waveforms with the grid side currents, as shown in Fig. 12 (d). The WT side AC currents shown in Fig. 12 (c) remain balanced. These results do not exhibit significant overvoltage on the healthy phases nor excessive overcurrent. Fig. 12 (f) and (g) show that the MMC DC side does not exhibit second order oscillation during faults with the proposed control. As the positive sequence voltage and current are both reduced due to the fault, the power transferred to the onshore grid is also decreased as shown in Fig. 12 (f). The offshore MMC arm currents shown in Fig. 12 (h) do not increase significantly and remain well below the safe limit of 1.2 pu [26]. Similarly, the submodule capacitor voltages exhibit some disturbances during the fault but the maximum over-voltage is limited to 20% during the transients [27, 28].

Table 1 The time sequence for single-phase-to-ground fault

Events	Fault occurs	Injecting negative sequence current	Fault cleared	Negative sequence voltage <5%
Time	2.5 s	2.5-2.64s	2.64s	2.71s

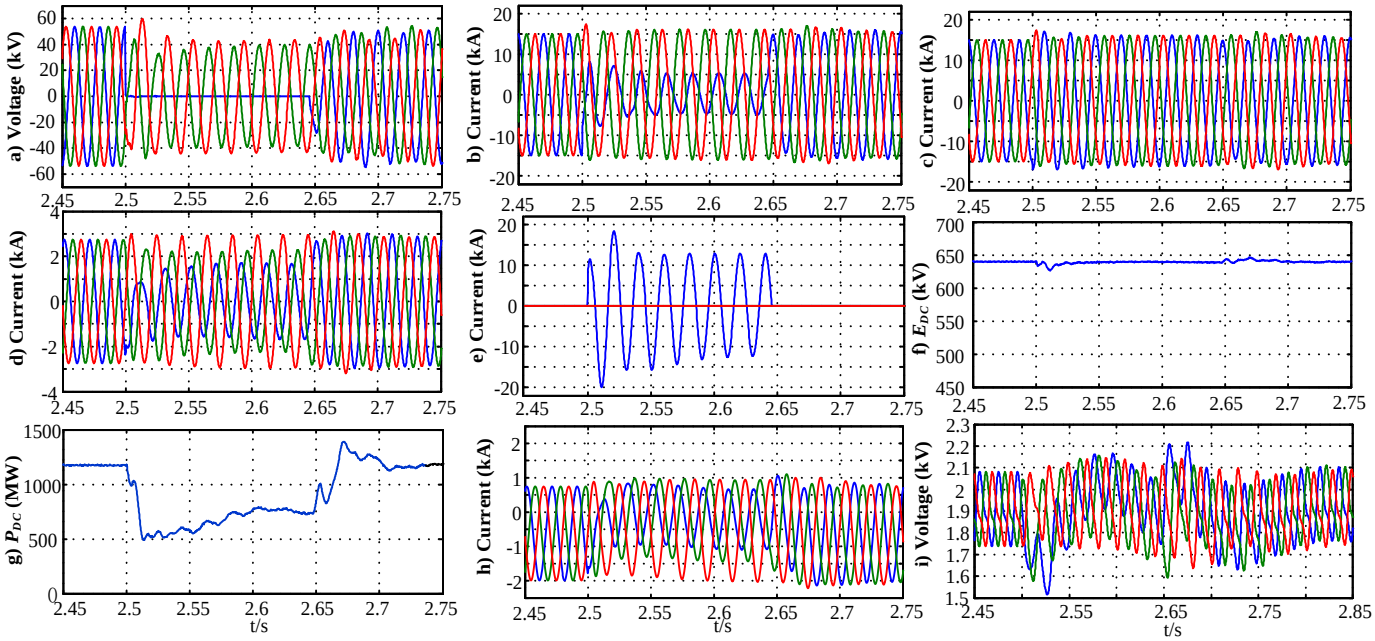

Fig. 12 Simulation waveforms during single-phase-to-ground fault: (a) offshore MMC AC voltages (E_{MMC}), (b) and (c) are AC currents injected into offshore network by the offshore MMC (I_{MMC}) and WTs (I_{WT}), respectively, (d) MMC converter side currents, (e) fault current (I_F), (f) DC side voltage (E_{DC}), (g) DC side power (P_{DC}), (h) MMC upper arm currents, (i) MMC average capacitor voltages

Fig. 13 illustrates the speeds of system voltage recovery under two different injected negative sequence currents of 0.1 and 0.25 pu. When injecting 0.1 pu negative sequence current, it takes around 200 ms after fault clearance for the offshore negative sequence voltage to reduce to below 5%. In contrast, the increase of the negative sequence current to 0.25 pu enables

the system voltage to restore more quickly, and the recovery time is reduced to 60 ms.

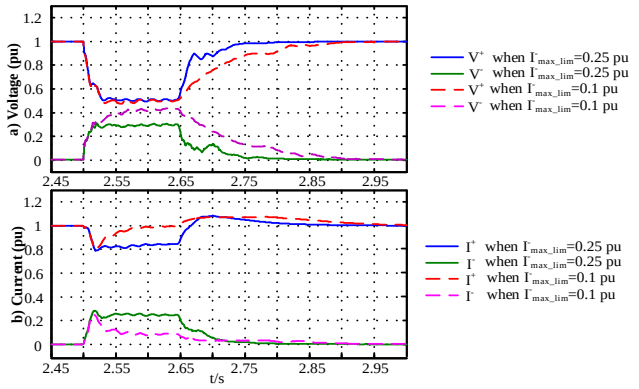

Fig. 13 Influence of injected negative sequence current amplitude on system recovery speed: (a) positive and negative sequence voltages, (b) positive and negative sequence currents.

B. *Phase-to-phase AC faults*

Table 2 The time sequence for phase-to-phase fault

Events	Fault occurs	Injecting negative sequence current	Fault cleared	Negative sequence voltage <5%
Time	2.5 s	2.5-2.64s	2.64s	2.71s

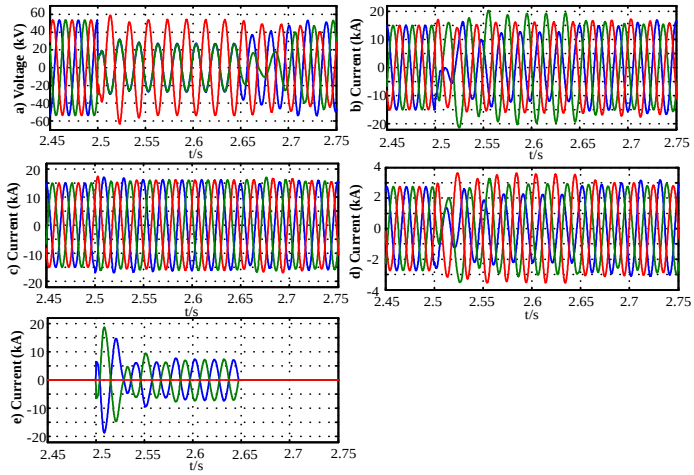

Fig. 14 Simulation waveforms for the scenario during phase-to-phase (*a*-*b*) fault: (a) offshore MMC AC voltages (E_{MMC}), (b) and (c) are AC currents for the offshore MMC (I_{MMC}) and WTs (I_{WT}) injected into offshore network, respectively, (d) MMC converter side currents, (e) fault current (I_F).

Fig. 14 summarizes simulation waveforms for a phase-to-phase AC fault when offshore MMC injects controlled negative sequence currents to accelerate AC voltage recovery, while WT converters control their negative sequence currents at zero. The time sequence of events during the fault is listed in Table 2.

Fig. 14 (a) to (e) confirm that the proposed scheme ensures speedy AC voltage recovery (around 60 ms) in post-fault, with the MMC currents remaining tightly controlled. Also, the supplied fault currents remain well-regulated and can be adjusted accordingly to facilitate fault detection and prevent overvoltage.

C. *Phase-to-phase-to-ground AC faults*

Fig. 15 summarizes simulation waveforms for a phase-to-phase-to-ground AC fault with the time sequence of events listed in Table 3. These plots indicate that the offshore AC voltage start to recover to pre-fault condition as soon as the fault is cleared. As shown in Fig. 15 (a), the overvoltage of the healthy phase during the fault is effectively suppressed by actively reducing the positive sequence voltage according to (21), which considers both the negative and zero sequence voltages. If desired, the magnitude of the fault current in Fig. 15 (e) can be further reduced by instructing the MMC to reduce the magnitude of the positive sequence voltage, as aforementioned in section II C.

Table 3 The time sequence for phase-to-phase–to-ground fault

Events	Fault occurs	Injecting negative sequence current	Fault cleared	Negative sequence voltage <5%
Time	2.5 s	2.5-2.64s	2.64s	2.71s

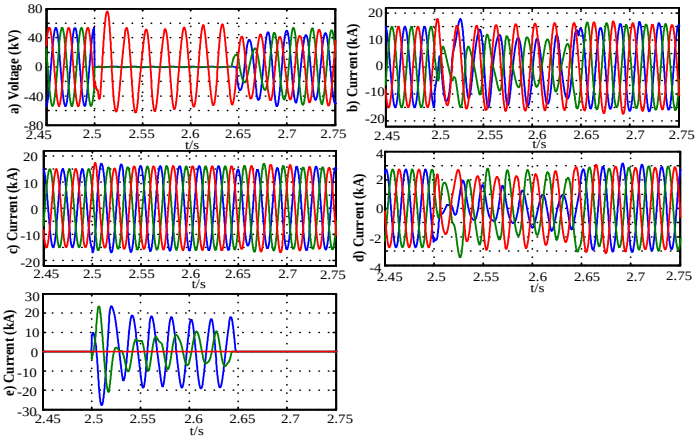

Fig. 15 Simulation waveforms during phase-to-phase-to-ground AC fault: (a) offshore MMC AC voltages (E_{MMC}), (b) and (c) are AC currents for the offshore MMC (I_{MMC}) and WTs (I_{WT}) injected into offshore network, respectively, (d) MMC converter side currents, (e) fault current (I_F).

V. Example Illustration of Potential Application of the Proposed Control Method

The proposed control strategy also simplifies protection arrangement against offshore asymmetric AC faults. For example, when an asymmetric AC fault F_2 occurs on the cable C1 as shown in Fig. 11, according to the discussions and analysis presented earlier, the current distribution in the offshore AC network can be summarized as follows:

- As WT converters do not inject negative current (fault current), no overcurrent will be observed in WT converters and the cables associated with healthy clusters and their respective ACCBs (CB2, CB3 and CB4, Fig. 11).
- Only the AC cable and circuit breaker CB1 in the faulty cluster will experience overcurrent, dominantly due to additional negative sequence current provided by the offshore MMC, i.e. AC cable C5 and part of cable C1 in the fault current path. No extra current stress will be exerted on part of C1 associated with the WTs. Thus, the current in CB1 can be expressed as:

$$I_{CB1}^{abc} = I_{WT1}^{abc} - I_{F2}^{abc}. \quad (22)$$

Notice (22) reveals that the current in CB_1 consists of positive sequence current from WT converters which is limited to 1.1 pu, and negative sequence current from the offshore MMC.

To substantiate the above discussion, the permanent single-phase-to-ground fault F_2 is simulated. The ACCBs are opened with a fixed delay of 7 cycles then clear the fault at next zero crossing point. As articulated throughout the paper, the injected negative sequence current by the MMC is set at 0.25 pu, which determines the fault current level. In practical system, the setting of the negative sequence current threshold will be decided by the protection system requirements.

The simulation results as shown in Fig. 16 support the above analysis. No overcurrent is observed from healthy clusters as depicted in Fig. 16 (d), (f) and (h), with their peaks limited to 1.1 pu as stated earlier. In contrast, Fig. 16 (b) shows the currents flowing through CB1 of the fault cluster has exceeded 2.0 pu and has led to its tripping. Following the fault isolation, the faulty cluster is shut down and the remaining parts of the offshore grid regain their steady-state conditions, see Fig. 16 (a) and (c).

The proposed control method can be further enhanced by gradually ramping up the MMC negative sequence current, controlling both current tripping threshold and time based on specific protection requirements. This feature can be used to reduce the circuit breaker ratings at cluster and string levels, thereby the total cost.

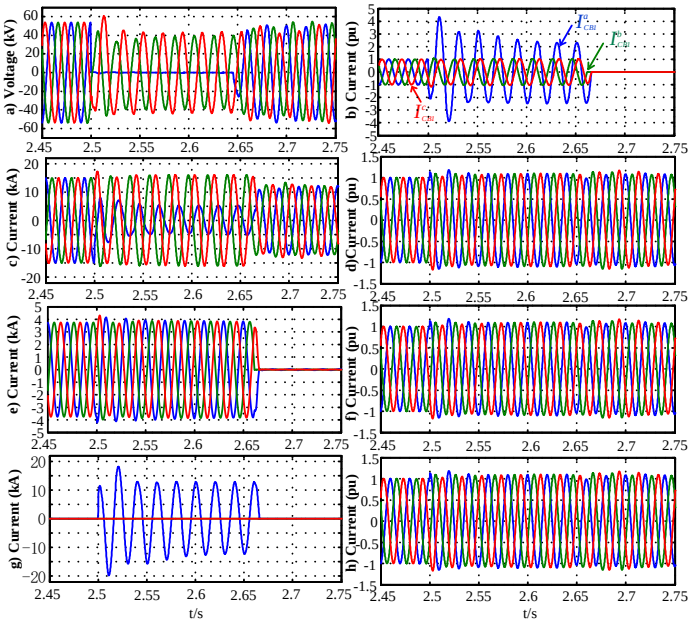

Fig. 16 Overcurrent protection waveforms during cluster fault: (a) grid side voltage (E_{MMC}), (b), (d), (f) and (h) are currents for CB1-4 (I_{CB1}, I_{CB2}, I_{CB3}, I_{CB4}) in pu, (c) MMC grid side currents (I_{MMC}), (e) WT currents of the faulty cluster (I_{WT1}), (g) fault currents (I_F).

VI. Conclusions

This paper has conducted a comprehensive study on possible ways in which the positive, negative and zero sequence currents and voltages could be controlled during asymmetrical AC faults in offshore AC collection networks of HVDC connected wind farms. Detailed studies presented in this paper reveal that, when negative sequence current is completely suppressed to zero during asymmetrical faults, the induced negative sequence voltage does not allow recovery of the AC voltage to the pre-fault condition. Such behavior would make protection system unable to distinguish between the fault and post-fault conditions. Therefore, this paper proposes a new modified control scheme that employs negative sequence voltage controller to facilitate controlled injection of negative sequence currents to not only define a safe level of fault current but also instigate immediate recovery of the AC voltage following clearance of AC faults. The excessive overvoltage in the healthy phases during asymmetrical AC faults is prevented by modifying the setting of the positive sequence voltage reference for the grid forming offshore HVDC converter, which takes the induced negative and zero sequence voltages into consideration. A case study, which utilizes the proposed control method to set up the overcurrent protection system for cluster cables, are also presented. The viability of the proposed control has been tested and confirmed using simulation performed in PSCAD.

VII. References

[1] I. Erlich, T. Neumann, F. Shewarega, P. Schegner, and J. Meyer, "Wind turbine negative sequence current control and its effect on power system protection," *in IEEE Power & Energy Society General Meeting*, 21-25 July 2013.

[2] P. Bresesti, W. L. Kling, R. L. Hendriks, and R. Vailati, "HVDC Connection of Offshore Wind Farms to the Transmission System," *IEEE Transactions on Energy Conversion*, vol. 22, pp. 37-43, 2007.

[3] M. H. Rahman, L. Xu, and L. Yao, "Protection of large partitioned MTDC Networks Using DC-DC converters and circuit breakers," *Protection and Control of Modern Power Systems*, vol. 1, p. 19, 2016.

[4] L. Xu, B. R. Andersen, and P. Cartwright, "VSC transmission operating under unbalanced AC conditions - analysis and control design," *IEEE Transactions on Power Delivery*, vol. 20, pp. 427-434, 2005.

[5] S. Alepuz, S. Busquets-Monge, J. Bordonau, J. A. Martinez-Velasco, C. A. Silva, J. Pontt, *et al.*, "Control Strategies Based on Symmetrical Components for Grid-Connected Converters Under Voltage Dips," *IEEE Transactions on Industrial Electronics*, vol. 56, pp. 2162-2173, 2009.

[6] C. H. Ng, L. Ran, and J. Bumby, "Unbalanced-Grid-Fault Ride-Through Control for a Wind Turbine Inverter," *IEEE Transactions on Industry Applications*, vol. 44, pp. 845-856, 2008.

[7] D. Roiu, R. I. Bojoi, L. R. Limongi, and A. Tenconi, "New Stationary Frame Control Scheme for Three-Phase PWM Rectifiers Under Unbalanced Voltage Dips Conditions," *IEEE Transactions on Industry Applications*, vol. 46, pp. 268-277, 2010.

[8] T. Neumann, T. Wijnhoven, G. Deconinck, and I. Erlich, "Enhanced Dynamic Voltage Control of Type 4 Wind Turbines During Unbalanced Grid Faults," *IEEE Transactions on Energy Conversion*, vol. 30, pp. 1650-1659, 2015.

[9] J. Jia, G. Yang, and A. H. Nielsen, "A Review on Grid-Connected Converter Control for Short-Circuit Power Provision Under Grid Unbalanced Faults," *IEEE Transactions on Power Delivery*, vol. 33, pp. 649-661, 2018.

[10] M. M. Shabestary and Y. A. I. Mohamed, "Asymmetrical Ride-Through and Grid Support in Converter-Interfaced DG Units Under Unbalanced Conditions," *IEEE Transactions on Industrial Electronics*, vol. 66, pp. 1130-1141, 2019.

[11] S. K. Chaudhary, R. Teodorescu, P. Rodriguez, P. C. Kjaer, and A. M. Gole, "Negative Sequence Current Control in

Wind Power Plants With VSC-HVDC Connection," *IEEE Transactions on Sustainable Energy*, vol. 3, pp. 535-544, 2012.

[12] A. Moawwad, M. S. E. Moursi, and W. Xiao, "A Novel Transient Control Strategy for VSC-HVDC Connecting Offshore Wind Power Plant," *IEEE Transactions on Sustainable Energy*, vol. 5, pp. 1056-1069, 2014.

[13] M. Ndreko, M. Popov, A. A. v. d. Meer, and M. A. M. M. v. d. Meijden, "The effect of the offshore VSC-HVDC connected wind power plants on the unbalanced faulted behavior of AC transmission systems," *in IEEE International Energy Conference (ENERGYCON)*, 4-8 April 2016.

[14] R. Li, L. Yu, and L. Xu, "Offshore AC Fault Protection of Diode Rectifier Unit-Based HVdc System for Wind Energy Transmission," *IEEE Transactions on Industrial Electronics*, vol. 66, pp. 5289-5299, 2019.

[15] Q. Tu, Z. Xu, Y. Chang, and L. Guan, "Suppressing DC Voltage Ripples of MMC-HVDC Under Unbalanced Grid Conditions," *IEEE Transactions on Power Delivery*, vol. 27, pp. 1332-1338, 2012.

[16] J. Wang, J. Liang, C. Wang, and X. Dong, "Circulating Current Suppression for MMC-HVDC under Unbalanced Grid Conditions," *IEEE Transactions on Industry Applications*, vol. 53, pp. 3250-3259, 2017.

[17] G. P. Adam, I. Abdelsalam, J. E. Fletcher, G. M. Burt, D. Holliday, and S. J. Finney, "New Efficient Submodule for a Modular Multilevel Converter in Multiterminal HVDC Networks," *IEEE Transactions on Power Electronics*, vol. 32, pp. 4258-4278, 2017.

[18] P. M. Anderson, *Analysis of faulted power systems [by] Paul M. Anderson*. Ames: Iowa State University Press, 1973.

[19] O. Goksu, N. A. Cutululis, P. S⊘rensen, and L. Zeni, "Asymmetrical fault analysis at the offshore network of HVDC connected wind power plants," *in IEEE Manchester PowerTech*, 18-22 June 2017.

[20] A. Abdalrahman and E. Isabegovic, "DolWin1 - Challenges of connecting offshore wind farms," *in IEEE International Energy Conference (ENERGYCON)*, 4-8 April 2016.

[21] N. R. Merritt, C. Chakraborty, and P. Bajpai, "New Voltage Control Strategies for VSC-Based DG Units in an Unbalanced Microgrid," *IEEE Transactions on Sustainable Energy*, vol. 8, pp. 1127-1139, 2017.

[22] D. Guo, M. H. Rahman, G. Adam, L. Xu, A. Emhemed, G. M. Burt, *et al.*, "Detailed quantitative comparison of half-bridge modular multilevel converter modelling methods," *in The 14th IET International Conference on AC and DC Power Transmission (ACDC 2018)*, 28-30 June 2018.

[23] R. Zeng, L. Xu, L. Yao, and D. J. Morrow, "Precharging and DC Fault Ride-Through of Hybrid MMC-Based HVDC Systems," *IEEE Transactions on Power Delivery*, vol. 30, pp. 1298-1306, 2015.

[24] P. Ruffing, N. Collath, C. Brantl, and A. Schnettler, "DC Fault Control and High-Speed Switch Design for an HVDC Network Protection Based on Fault-Blocking Converters," *IEEE Transactions on Power Delivery*, vol. 34, pp. 397-406, 2019.

[25] O. Goksu. "D3.2 Specifications of the control strategies and the simulation test cases", Report of the project 'PROgress on Meshed HVDC Offshore Transmission Networks' (PROMOTioN) funded by the European Union's Horizon 2020 research and innovation programme. [Online]. Available: https://www.promotion-offshore.net/fileadmin/PDFs/D3.2_Specifications_Control_strategies_and_simulation_test_cases.pdf, 2017.

[26] R. Li, L. Xu, and L. Yao, "DC Fault Detection and Location in Meshed Multiterminal HVDC Systems Based on DC Reactor Voltage Change Rate," *IEEE Transactions on Power Delivery*, vol. 32, pp. 1516-1526, 2017.

[27] K. Tahata, R. Uda, K. Kuroda, K. Kikuchi, R. Yamamoto, H. Ito, *et al.*, "Mitigation on requirement of DCCB by DC reactor for multi-terminal HVDC operation," *in The 12th IET International Conference on AC and DC Power Transmission (ACDC 2016)*, 28-29 May 2016.

[28] G. Zou, Q. Huang, S. Song, B. Tong, and H. Gao, "Novel transient-energy-based directional pilot protection method for HVDC line," *Protection and Control of Modern Power Systems*, vol. 2, p. 15, 2017.

Lei Shi received the B.Sc. degree with first class honour from University of Strathclyde, Glasgow, U.K., in 2016. He is currently pursuing the Ph.D. degree in Electronic & Electrical Engineering, University of Strathclyde, Glasgow, U.K.

His research interests include HVDC transmission system and offshore windfarm system.

Grain P. Adam (M'12) received the B.Sc. and M.Sc. degrees (Hons.) from Sudan University for Science and Technology, in 1998 and 2002 respectively; and a PhD in Power Electronics from University of Strathclyde in 2007.

He is a researcher with University of Strathclyde in Glasgow, UK, since 2008. His research interests are fault tolerant voltage source converters for HVDC applications; modelling and control of HVDC transmission systems and multi-terminal HVDC networks; voltage source converter based FACTS devices; and grid integration issues of renewable energies.

Dr. Adam has authored and co-authored several technical reports, and over 100 journal and conference articles. Dr. Adam has published two books in applications of power electronics in power systems and renewable energy. He is an active contributor to reviewing process for several IEEE and IET Transactions, Journals and conferences, and a member of IEEE. He is an Associate Editor of Journal of Emerging and Selected Topics in Power Electronics.

Rui Li received the M.S. and Ph.D degrees in electrical engineering from Harbin Institute of Technology, Harbin, China, in 2008 and 2013, respectively. He is a researcher with University of Strathclyde in Glasgow, UK, since 2013.

His research interests include HVDC transmision system, grid integration of renewable power, power electronic converters, and energy conversion.

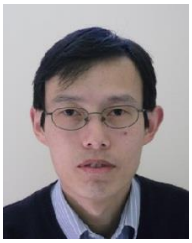

Lie Xu (M'03–SM'06) received the B.Sc. degree in Mechatronics from Zhejiang University, Hangzhou, China, in 1993, and the Ph.D. degree in Electrical Engineering from the University of Sheffield, Sheffield, UK, in 2000.

He is currently a Professor at the Department of Electronic & Electrical Engineering, University of Strathclyde, Glasgow, UK. He previously worked in Queen's University of Belfast and ALSTOM T&D, Stafford, UK. His research interests include power electronics, wind energy generation and grid integration, and application of power electronics to power systems. He is an Editor of IEEE Transactions on Power Delivery and IEEE Transactions on Energy Conversion.